DC Railway System Emulator for Stray Current and Touch Voltage Prediction

Amr Ibrahem, Ali Elrayyah, Yilmaz Sozer, *Senior Member, IEEE*, and J. Alexis De Abreu-Garcia, *Member, IEEE*

***Abstract*—A system to emulate railway dc systems is presented in this paper. The emulator is designed to simulate the behavior of railway systems in terms of stray currents and touch voltages. Power electronics circuits are used as variable resistors to simulate the train motion. The emulator provides a test bed to not only study and analyze the effects of stray currents and touch voltages, but also to evaluate techniques that mitigate these effects before they are physically implemented. The proposed emulator system is verified through simulation studies and hardware experimentations.**

***Index Terms*—DC power systems, power electronics, rail transportation power systems, rail transportation testing, simulation.**

I. Introduction

In DC rail transit systems, the running rails are usually used as conductors to carry the traction current. This arrangement is considered for economic purposes since it eliminates the need to install special current carrying conductors. However, a significant part of the return current could leak into the ground in parts of the system with poor insulation [1], [2]. The amount of leakage current depends mainly on the conductance of the return tracks compared to that of ground, the quality of the insulation between the tracks and the earth, and the train current, which in turn depends on the train operating conditions (accelerating, braking, etc.)

While stray current does not normally affect the railway electric system, it can cause serious damage to the metallic structures located near the railway tracks by accelerating the corrosion process on them. For example, corrosion could reduce the lifetime of underground cables and pipelines located near the transit system. According to [3]–[5], the annual cost of corrosion caused by transit system stray currents to the U.S. economy is estimated to be about $500 million.

Since the value of the running rail resistance could be as high as several tens of milliohms per kilometer, and since the train's drawn currents could reach up to 1200 A, a significant voltage drop (60–100 V) on the running rail could be generated underneath the train. Therefore, railway systems may pose a seriously hazardous situation for human lives' as the touch voltage increases when the train current becomes very high [1], [6], [7]. Further, since the stray current leaks throughout the rail lines, the peak of the touch voltage usually occurs at the train location.

Many methods have been developed to measure and control both the stray current and the touch voltage; however, it is very costly, difficult, and impractical to test these methods on an actual railway system. A leakage current control technique is proposed in [1] to limit the stray current and touch voltage by controlling the drive. Similar approach but different control strategies are proposed by other authors. The sensor is placed between the return path and the earth ground to determine the leakage current. The control algorithm operates to limit the leakage current within the limits. Here, it is very difficult to test the control algorithm and see its effectiveness on the real system. It is not easy to get into the field to do these tests. It requires taking the units out of the service for the safety of the passengers which is also very expensive to run the system for testing the sensors. That is why it is desired to test the operation of the controller with the emulator. With the emulator it would be possible to change the impedances and see the response of the controller accordingly.

Therefore, there is a need for a low cost yet effective simulation test bed that would emulate the behavior of dc railway systems. This is especially so because it is always more expedient and cost effective to first investigate the behavior of the proposed methodologies using low-cost experimental setups prior to their implementation on an actual system.

This paper proposes an emulator for electrical railway systems which can simulate both the railway system and the train motion on it. The emulator can be used to obtain measurements of both the stray current and the touch voltage under different operating conditions. The emulator is built on electronic variable resistances, but the required impedances for the emulation have variable ranges as a function of the train position and the environmental conditions, depending on the placement of the impedances. This paper provides new architectures and the combination of them to make a system for railway system emulation. To the best of our knowledge, our research is the only research that looks at the requirement for the railway system emulations and realizes them with the experimental implementation. This emulator can, therefore, be used to propose and test different control schemes and to verify their efficiency.

Although there have been methods for determining the leakage currents at the negative side, there is not much research for determining the leakage current at the positive side. A new technique injects the high-frequency signal into the middle of the line segment and simultaneously blocks the injected signals at the sides of the segments. The impedance of the segment is

Manuscript received March 7, 2016; revised June 30, 2016; accepted August 15, 2016. Date of publication September 7, 2016; date of current version January 18, 2017. Paper 2016-TSC-0201.R1, presented at the 2015 IEEE Energy Conversion Congress and Exposition, Montreal, QC Canada, Sep. 20–24, and approved for publication in the IEEE Transactions on Industry Applications by the Transportation Systems Committee of the IEEE Industry Applications Society. This work was supported by the Transportation Research Board of the National Academies (TCRP Project D-17, FY 2013).

The authors are with the Electrical and Computer Engineering Department, The University of Akron, Akron, OH 44325 USA (e-mail: ai21@zips.uakron.edu; aelrayyah@qf.org.qa; ys@uakron.edu; alexis4@uakron.edu).

Color versions of one or more of the figures in this paper are available online at http://ieeexplore.ieee.org.

Digital Object Identifier 10.1109/TIA.2016.2606367

TABLE I
MAXIMUM STRAY CURRENT FOR DIFFERENT MODELING PATHS

# of ground paths	Current at 1 km (A)	Current at 3 km (A)	Current at 6 km (A)	Current at 10 km (A)
2	0.0265	0.5622	2.2449	6.2112
8	0.0265	0.5622	2.2457	6.2170
14	0.0265	0.5622	2.2458	6.2174
Current for infinite paths	0.0265	0.5622	2.2458	6.2176

then correlated to the leakage current at the positive side. The emulator that is developed in this paper would be used to test the performance of this type of sensors.

II. RAILWAY MODELING APPROACH

To model a railway electrical system, the resistance of the tracks and the resistances between the tracks and the ground are assumed to be uniformly distributed throughout the railway. The train is modeled as a current source whose current depends on the operating condition of the train, such as accelerating or braking.

The main challenge in modeling the stray current is the fact that it does not leak from specific points on the track; but rather, it leaks throughout the track. Therefore, the stray current may be treated in a similar way as the current of the power system transmission lines, where the voltage and the current at a point x on the line [4], [8], [9] are given by

$$i\,(x) \;= C_1 e^{yx} + \; C_2 e^{-yx} \tag{1}$$

$$u\,(x) \;= -R_0 (C_1 e^{yx} + \; C_2 e^{-yx}) \tag{2}$$

for $0 < \; x \; < 1 \; y = \sqrt{R/R_G} \; R_O \; = \sqrt{R R_G}$ where $u(x)$ represents the potential of the conductor at point x, $i(x)$ is the current in the conductor at point x, R is the longitudinal resistance of the conductor (ohm/km), and R_G is the leakage resistance between the conductor and ground (ohm–km).

Equations (1) and (2) provide the exact amount of current and touch voltage at any point x on the line. However, it is impractical to implement them using physical hardware as it requires an infinite number of paths to ground [10]–[12]. In the case of a railway system emulator, the length of the conductor is not very long as the typical distance between any two stations in a railway system is within 3–8 km. Therefore, with a limited number of paths to ground, an approximate model can be obtained. As explained in [3], [13], and [14], the highest value of the stray current for a grounded system is given by

$$I_{\text{stray}} = \frac{I \; R \; l^2}{2 \; R_G} \tag{3}$$

where I is the train current, and l is the distance between every two stations. To determine the number of ground paths that would be sufficient to obtain a model, that is accurate enough and feasible for practical implementation, a comparison study was conducted. This study yielded the results listed in Table I. In this table, the maximum stray current was obtained for different ground paths and different distances between the stations. The currents using an infinite number of paths are calculated using (1).

From Table I, it is clear that the maximum values of the stray current differ from the exact current at station lengths of 6 and 10 km with a percentage error in both cases of less than 0.001. Clearly, since in a typical railway system, the distance between two stations is less than 6 km, only two paths to ground turn out to be sufficient to effectively simulate grounded railway systems. This leads to the model structure shown in Fig. 1.

III. VARIABLE IMPEDANCE EMULATOR

To emulate the train moving along the line, variable resistors are included in the model shown in Fig. 1. When the train is moving from station 1 to station 2, the values of R_1 and R_3 increase, while the values of R_2 and R_4 decrease. Similarly, the value of R_{G2} will decrease, while that of R_{G1} will increase. The main challenge in representing these resistors is the large difference between the values of the track resistance and the ground resistance. While the track resistance (R_1, R_2, R_3, and R_4) is typically between 0.02 Ω and 0.08 Ω/km, the resistance between the ground and the track (R_{G1} and R_{G2}) is between 60 to 100 Ω/km. Accordingly, two separate power electronics circuits would be required to emulate the high and low resistances of the railway system.

A. Variable High-Resistance Emulation Circuit (VHR-EC)

We propose to have two types of converters to emulate different range of the resistances. The topology of the proposed VHR-EC converter type used to emulate the high resistance, which represents the ground to earth resistance, is shown in Fig. 2. The proposed topology includes the resistance R_{in} in conjunction with the boost converter. The voltage across the converter can be controlled to mimic the line impedance effects. The duty ratio of the converter is then adjusted to emulate the various line impedances. When the duty ratio is zero, the emulated resistor will equal R_{in}, but when the duty ratio is one, R_{in} will be shorted, and, thus, the emulated resistance will be almost zero. IGBTs are used in the converter circuitry provided in Fig. 2. The duty ratio of the converter is controlled in a closed-loop fashion by the digital signal processor to generate an effective resistance between the ports of the converter. The converter actually reduces the effective resistance as a function of the actual resistance provided at the converter input and duty ratio.

Fig. 3 shows the relationship between the duty ratio and the resistance for different values of R_{in}. One possible limitation of this configuration is its inability to accurately represent very small resistances as the internal resistances of the circuit components would affect their accuracy. However, since the track-to-ground resistances are usually large, this limitation does not affect the performance of the VHR-EC in this case, and, thus, the method can be used for generating relatively high resistances. For emulating low resistances, this method is not viable, as the internal resistances of the IGBTs will impact the resultant resistance to be emulated.

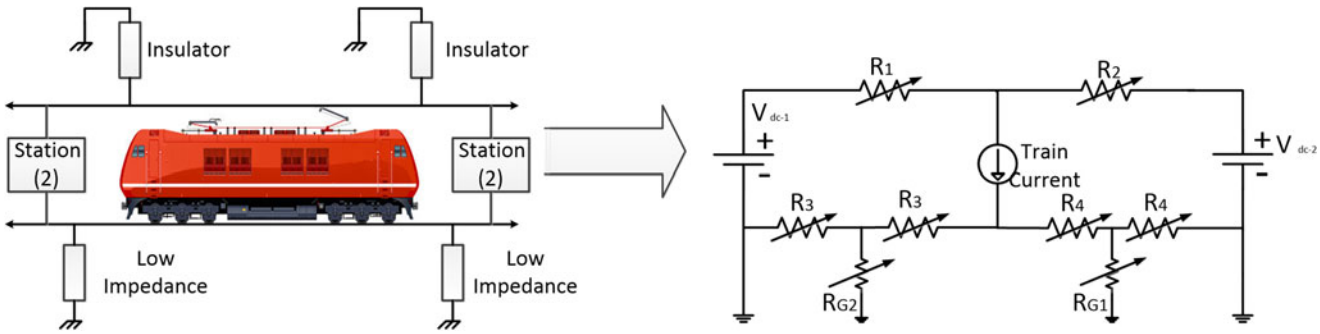

Fig. 1. Impedance model of the railway system.

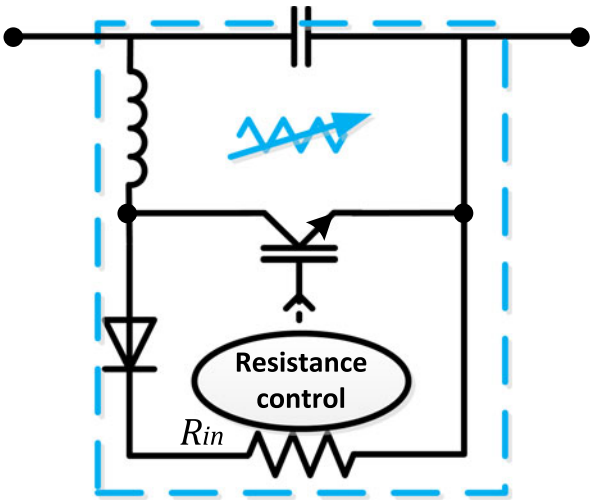

Fig. 2. Circuit diagram of the VHR-EC.

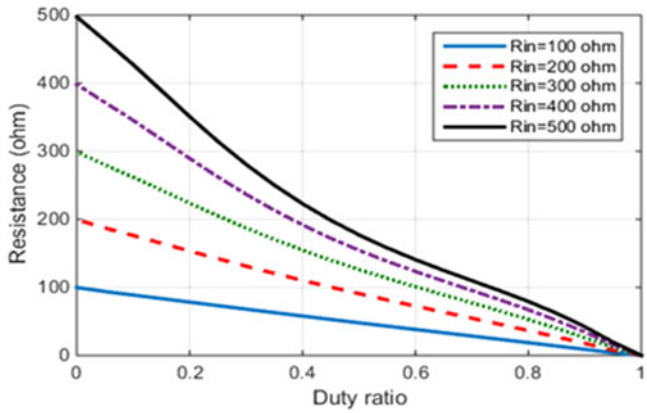

Fig. 3. Relationship between duty ratio and resistance for VHR-EC.

The values of the inductor and the capacitor in the emulator must be designed so as to reduce the ripple in the voltage and current in the converter, which will reduce the ripple in the output resistor. Since the VHR-EC behaves as a boost circuit it follows that

$$\Delta I_L = \frac{V_c D}{f\ L} \tag{4}$$

$$\Delta V_C = \frac{V_c D}{fRC\,(1\ -\ D)}\ . \tag{5}$$

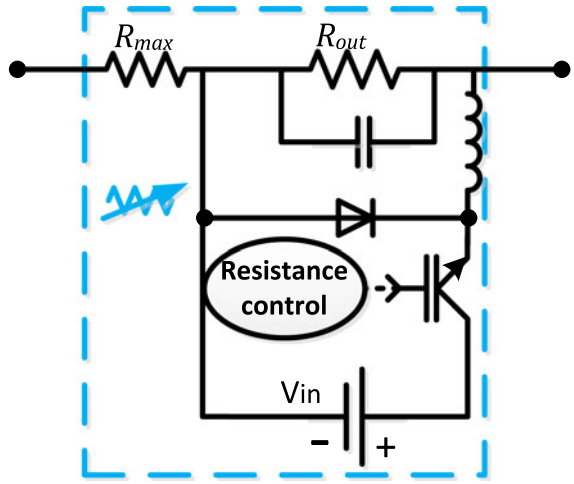

Fig. 4. Circuit diagram of the VLR-EC.

In general, to reduce the ripple in the VLR-EC output impedance, both the ripple of the input voltage and current must be reduced. However, considering that V_C is the touch voltage and I_L is the stray current, we found that when $V_C >> I_L$, we can assume

$$\Delta R \propto \Delta V_C = \frac{V_c D}{fRC\,(1\ -\ D)} \tag{6}$$

where *R* is the VHR-EC impedance, V_C is the capacitor voltage, *D* is the duty ratio, f is the switching frequency, and *L* and *C* are the inductor and capacitor values used in the VHR-EC. These values should be chosen to meet the required resistance ripple.

B. Variable Low-Resistance Emulation Circuit (VLR-EC)

Although the rail-to-the-ground impedances are high, the line impedances of the railway are quite low. Thus, the internal impedances of the emulator proposed in Fig. 2 would impact the emulation accuracy for low impedances. To represent the low resistances of the track resistor, resistances $R_{\rm out}$ and $R_{\rm max}$ associated with the buck converter are proposed as shown in Fig. 4. The output of the converter is the resistor connected to the track path that carries the train current. IGBTs are used in this configuration. Their switching times are controlled in a closed-loop fashion by the digital signal processor to generate an effective resistance between the ports of the converter.

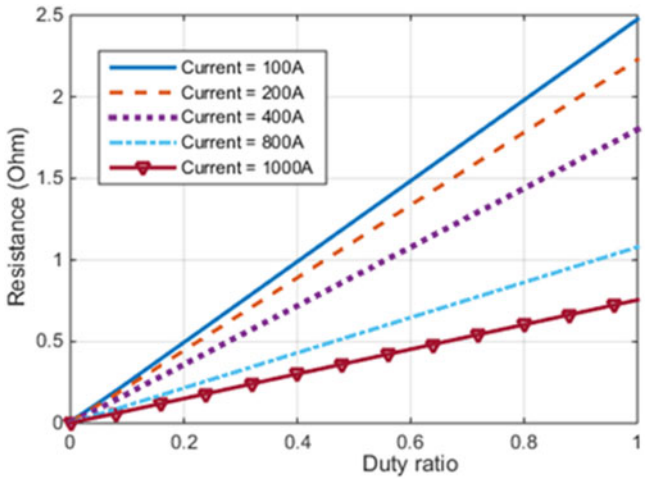

Fig. 5. Relationship between resistance and voltage for VLR-EC.

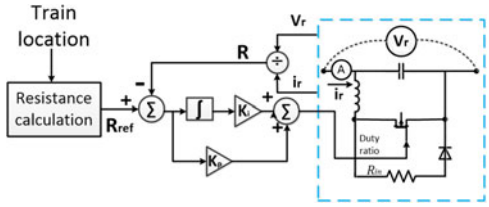

Fig. 6. Control block diagram of the VHR-EC.

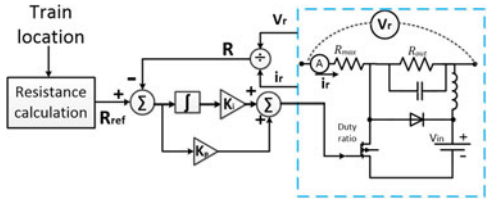

Fig. 7. Control block diagram of the VLR-EC.

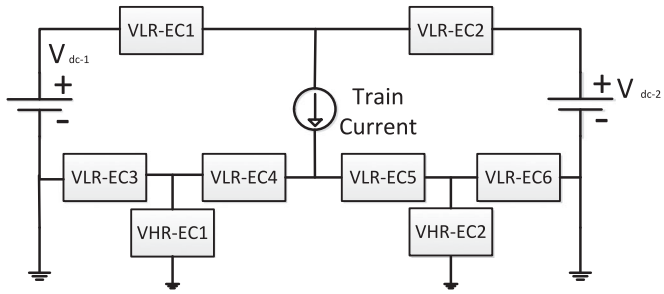

Fig. 8. Impedance model of the railway system using the variable impedance emulator.

Since the train is represented by a current source with a known current value, by changing the duty ratio, the voltage across the resistor $R_{\rm out}$ will change; this will in turn affect the value of the total track resistance. $R_{\rm max}$ represents the maximum resistance, as the controlled resistance portion emulated by the converter is always negative. To get good sensitivity, it is desirable to keep $R_{\rm max}$ low. The voltage across the converter ports will be affected by the train current which will impact the resultant resistance across the ports. Fig. 5 presents the resultant resistance across the ports of the converter as a function of the duty ratios at different train currents. The main limitation of this configuration is that a high voltage at the converter could be needed to represent a high range of resistances. However, for the application being considered here, this configuration is sufficient to give the required performance as it is used to represent low resistances.

Since VLR-EC behaves as a buck converter and as we only are concerned about the output resistance value here, we find that the resistance ripple is equal to the ripple in the output voltage of the converter, and thus

$$\Delta R \propto \Delta V_C = \frac{V_c\,(1\ -\ D)}{8LCf^2} \tag{7}$$

where *R* is the VLR-EC impedance and *L* and *C* are the inductor and capacitor values used in the VLR-EC. These values should be chosen to meet the required resistance ripple.

IV. Control of Variable Resistance Emulators

To control the variable resistor requires only a PI controller as the relationship between the resistance and the duty ratio, or voltage, is almost linear in both cases. The reference resistances for railway emulation can be determined as

$$R_2 = (D\ -\ T)\,R_o \tag{8}$$

$$R_4 = \frac{(D\ -\ T)\,R}{2} \tag{9}$$

$$R_{G1} = \frac{R_G}{D\ -\ T} \tag{10}$$

TABLE II
Parameters Values Used in the Simulation

I	R_o	R	R_G
1000 A	0.08 Ω/km	0.04 Ω/km	80 Ω/km
E	D	L	C
1100 V	4 km	5 mH	0.1 mF

where D is the distance between two stations, T is the distance between the train and Station 1, and R_o is the per km resistance of the overhead lines.

The controller provides the duty ratios for both the VHR-EC and the VLR-EC emulators. In order to avoid oscillations during start up, initial duty ratio values are programmed into a look-up table, as a function of the reference resistances. The PI controller picks up the latter to generate the required duty ratios. The block diagrams of the hardware and the control algorithms for VHR-EC and VLR-EC are presented in Figs. 6 and 7, respectively.

V. Simulation Results

The performance of the proposed emulator was analyzed using MATLAB/Simulink. The railway system in Fig. 1 was simulated using the proposed variable impedance circuits as shown in Fig. 8. Table II includes the simulation parameters used for this analysis. In this table, the variable *I* is the train current,

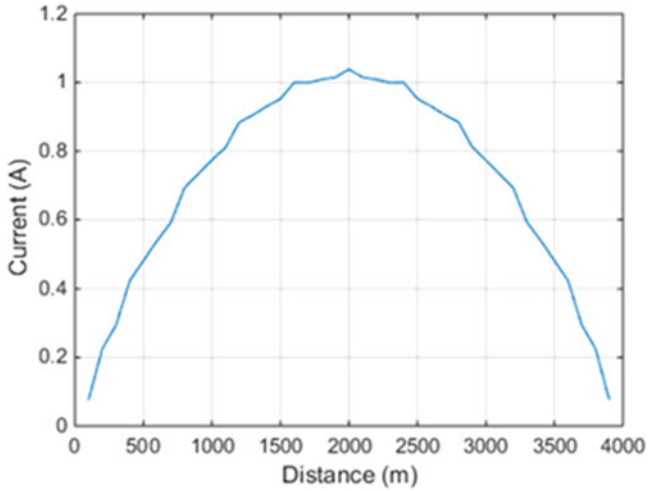

Fig. 9. Total stray current leaking from the rail as a function of the train distance from the substation.

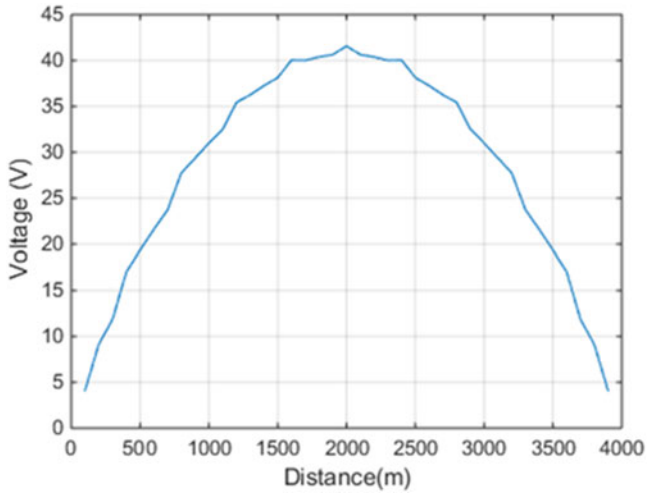

Fig. 10. Rail touch voltage as a function of the train distance from the substation.

R_O is the overhead line resistance, R is the resistance of the rail tracks, R_G is the resistance between the rail and ground, E is the railway system voltage, L and C are the inductance and capacitance used in the emulator, and D is the variable distance between the two stations. The impedances used for the emulations are based on the experimental field tests from the San Francisco Bay Area Rapid Transit District reported in [15] and [16]. Fig. 9 shows the total stray current leaking from the rail, Fig. 10 shows the touch voltage of the rail, and Fig. 11 shows the actual and the desired values of R_1.

As shown in Figs. 8 and 9, the touch voltage and the stray currents are maximums when the train is midway between the two stations. Letting the right and left return impedances from the train be R_A and R_B, respectively, and the total return impedances be R_T ($R_B = R_T - R_A$) allows us to write

$$V = I \times \left(\frac{R_A R_T - {R_A}^2}{R_T} \right)$$

where V is the touch voltage and I is the train current.

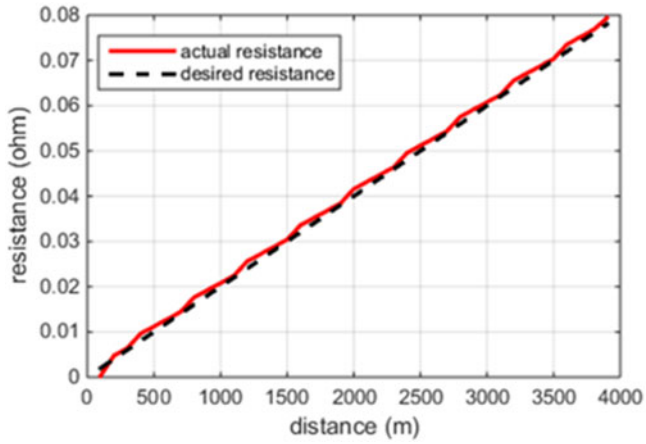

Fig. 11. Actual and desired value for R_1.

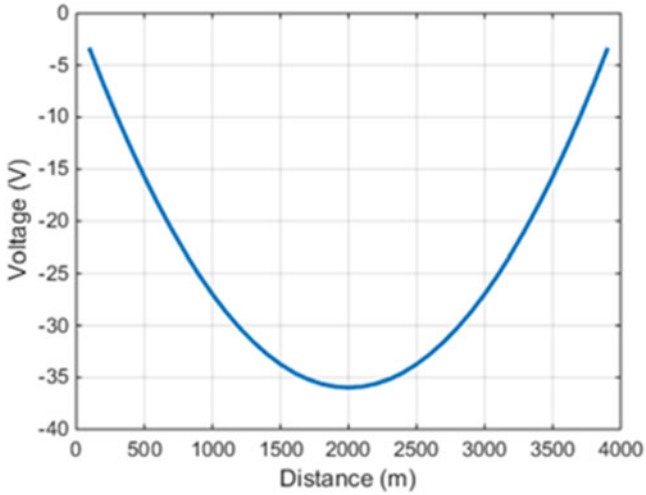

Fig. 12. Rail touch voltage as a function of the train distance from the substation (regenerative braking).

Setting the derivative of V with respect to R_A to 0 yields $R_A = \frac{R_T}{2}$, which is the case when the train is halfway between two stations.

The behavior of the stray current and the touch voltage of the system under regenerative braking is similar to that of normal operation with a negative polarity.

A regenerative brake is an energy recovery mechanism which converts kinetic energy into a form which can be either used immediately or stored until needed. This contrasts with conventional braking systems, where the excess kinetic energy is converted to unwanted and wasted heat by friction in the brakes. In addition to improving the overall efficiency of the vehicle, regeneration can greatly extend the life of the braking system as its parts do not wear as quickly. For the sake of simplicity we will assume that the acceleration time is equal to the braking time, with a factor of 0.9 that represents the losses in the system. In this case the train current is 900 A, and the other parameters are as listed in Table II.

Fig. 12 shows the total stray current leaking from the rail, while Fig. 13 shows the touch voltage of the rail under regenerative braking.

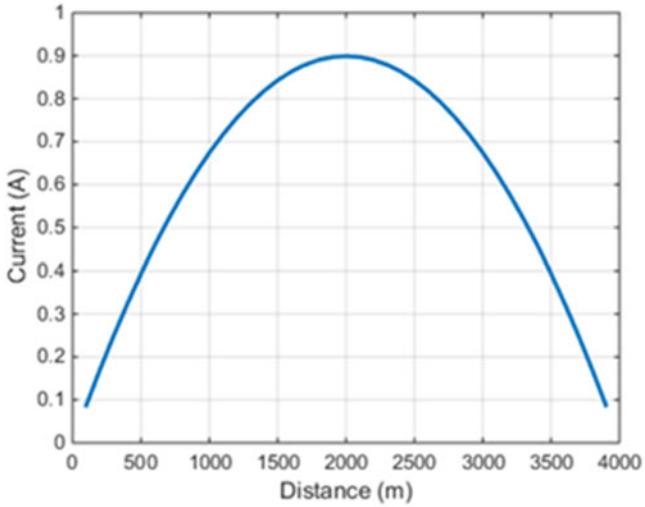

Fig. 13. Total stray current leaking from the rail as a function of the train distance from the substation (regenerative braking).

TABLE III
COMPONENT VALUES FOR THE VHR-EC MODULE

R_{in}	L	C
200 Ω	5 mH	0.1 mF

VI. EXPERIMENTAL RESULTS

The experiment was conducted for both impedance ranges to prove the validity of the proposed methods. Both the VHR-EC and VLR-EC hardware modules are controlled using a TI 28335 digital signal processor with a switching frequency of 20 kHz. The emulator is developed with the available modules at the University to experimentally verify the operating principles of the proposed topologies to emulate the variable resistances having different ranges and sensitivities. The unit can be scaled up to be used in rated operating conditions of the railway system. The impedance values used in the experimental emulator verifications are taken from the San Francisco Bay Area Rapid Transit District reported in [15] and [16].

A. For High Resistance

An experimental setup was built for the topology given in Fig. 2. The values of the passive elements were selected as listed in Table III.

R_{in} will be the maximum impedance of the variable resistor. This value can be obtained by selecting the duty ratio to be zero. L and C are used to smooth out the resulting resistance value, to make it more stable, and to reduce any ripple on it.

The current through and the voltage across the variable resistor were measured while changing the reference value for the variable resistor. Fig. 14 shows the current through and the voltage across the resistor. Using these voltage and current values, the resistance values were calculated and graphed in Fig. 15. As seen from Fig. 15, the VHR-EC is capable of generating the commanded resistances accurately with good transient capabilities.

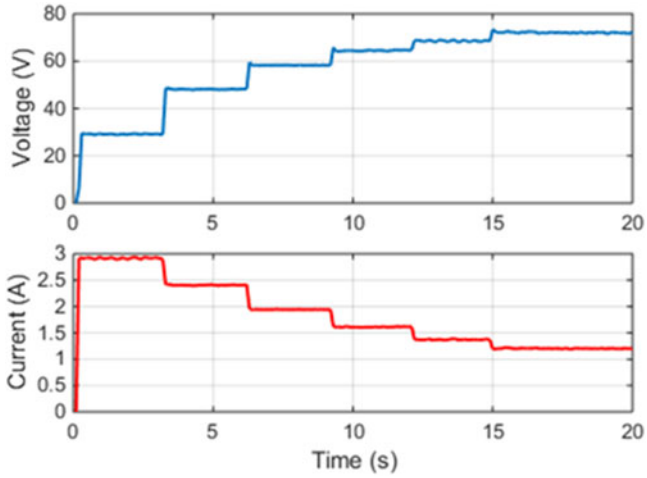

Fig. 14. Voltage across and current through the VHR-EC with different resistance commands.

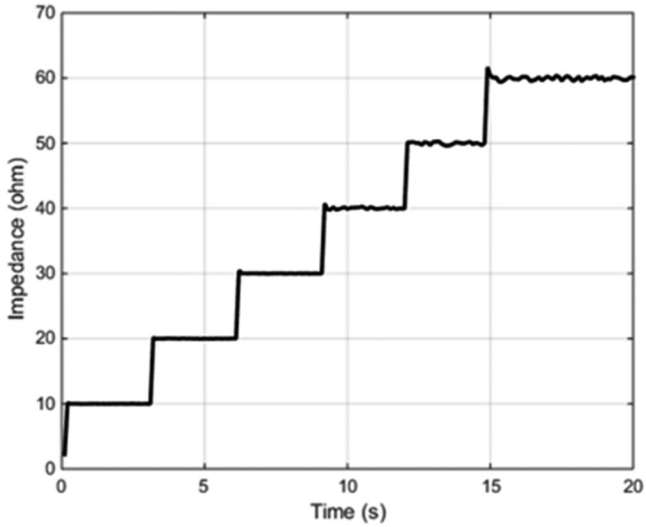

Fig. 15. Impedance of the VHR-EC with different resistance commands.

TABLE IV
COMPONENT VALUES FOR THE VLR-EC MODULE

R_{max}	R_{out}	V_{in}	L	C
4 Ω	10 Ω	20 V	5 mH	0.1 mF

B. For the Low Resistance

An experimental setup was built for the topology given in Fig. 4, using the values of the passive elements provided in Table IV.

R_{max} is chosen to be the maximum resistance. R_{out} is used to provide the negative voltage drop that will be used to change the variable resistance value. It is always better to have a large value of R_{out} to reduce the current drawn from the source. The

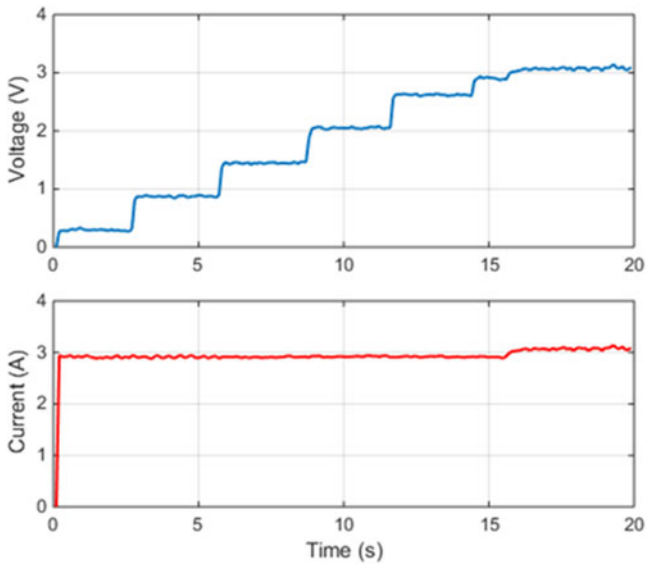

Fig. 16. Voltage across and current through the VLR-EC with different resistance commands.

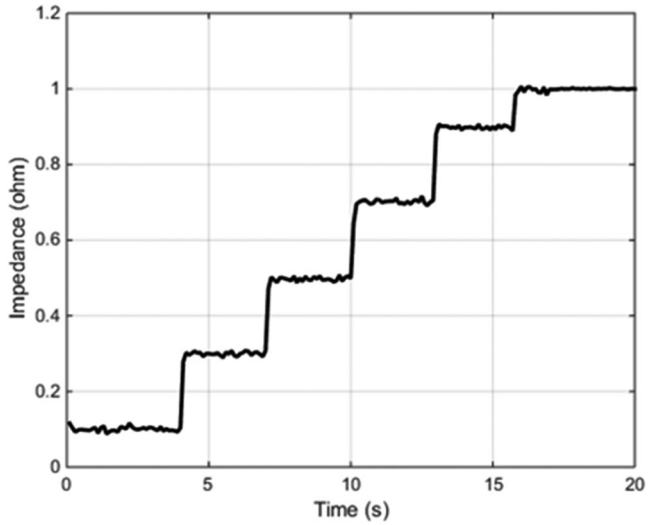

Fig. 17. Impedance of the VLR-EC with different resistance commands.

voltage across $R_{\rm out}$ is negative to achieve a negative resistance. The value of this voltage drop depends on the current in the circuit, but usually in this small range of resistance only a small voltage is needed. L and C are used to smooth out and stabilize the emulated resistance.

The current through and the voltage across the VLR-EC are measured and used to track the reference value for the variable resistor. Using the values of the voltage and current, the resulting impedance is calculated. The error between the reference and measured impedances drives the PI controller to generate the duty ratio for the VLR-EC module. Fig. 16 gives the voltage across and the current through the VLR-EC, with different resistance commands. The resultant resistances across the VLR-EC are presented in Fig. 17. As seen from Fig. 17, the VLR-EC is capable of generating the commanded resistances accurately with good transient capabilities.

VII. Conclusion

An electrical railway system, which is effective and feasible for practical implementations, was modeled to obtain the stray current and the touch voltage. Power electronics circuits were used as variable resistors to simulate the train movement between two stations. An emulator for a grounded railway system was designed, simulated, and experimentally verified. A boost converter, whose input is the ground resistance, was used to emulate high resistance values. A buck converter, whose output is a resistance in series with the track resistance, was used to emulate low resistance values. The proposed emulator, which was found to be effective in modeling the electrical behavior of the railway system, can be further developed to simulate floating systems. The emulator can be used to test methods of controlling and mitigating stray currents and touch voltages of the rail system.

References

[1] A. M. Niasati and A. Gholami, "Overview of stray current control in DC railway systems," in *Proc. Int. Conf. Railway Eng., Challenges Railway Transp. Inf. Age*, Hong Kong, Mar. 2008, pp. 1–6.

[2] L. Chien-Hsing and L. Chien-Jung, "Assessment of grounding schemes on rail potential and stray currents in a DC transit system," *IEEE Trans. Power Del.*, vol. 21, no. 4, pp. 1941–1947, Oct. 2006.

[3] C. A. Charalambous, I. Cotton, P. Aylott, and N. D. Kokkinos, "A holistic stray current assessment of bored tunnel sections of DC transit systems," *IEEE Trans. Power Del.*, vol. 28, no. 2, pp. 1048–1056, Apr.2013.

[4] J. G. Yu and C. J. Goodman, "Modelling of rail potential rise and leakage current in DC rail transit systems," in *Proc. IEE Colloq. Stray Current Effects DC Railways Tramways*, Oct. 1990, pp. 221–226.

[5] A. Zaboli, B. Vahidi, S. Yousefi, and M. M. Hosseini-Biyouki, "Evaluation and control of stray current in DC-electrified railway systems," *IEEE Trans. Veh. Technol.*, 2016, doi: 10.1109/TVT.2016.2555485.

[6] A. Ogunsola, A. Mariscotti, and L. Sandrolini, "Estimation of stray current from a DC-electrified railway and impressed potential on a buried pipe," *IEEE Trans. Power Del.*, vol. 27, no. 4, pp. 2238–2246, Oct.2012.

[7] Y. Cai, M. R Irving, and S. H Case "Iterative techniques for the solution of complex DC-rail-traction systems including regenerative braking," *IET Proc. Gener., Transm., Distrib.*, vol. 142, no. 5, pp. 445–452, Sep. 1995.

[8] J. E. Sankey and P. L. Anderson, "Effects of stray current on performance of metallic reinforcements in reinforced earth structures," *Transp. Res. Rec.*, vol. 1675, pp. 61–66, Jan. 2007.

[9] J. G. Yu, "The effects of Earthing strategies on rail potential and stray currents in DC transit railways," in *Proc. Int. Conf. Develop. Mass Transit Syst.*, London, Apr. 1998, pp. 303–309.

[10] J. Valero Rodríguez and J. Sanz Feito, "Calculation of remote effects of stray currents on rail voltages in dc railways systems," *IET Electr. Syst. Transp.*, vol. 3, no. 2, pp. 31–40, Jun. 2013.

[11] A. J. Davis, "Stray current control—An arbitrator's view," in *Proc. IET Colloq. Stray Current Effects DC Railways Tramways*, London, 1990, pp. 211–216.

[12] R. Natarajan, "Analysis of grounding systems for electric traction," *IEEE Trans. Power Del.*, vol. 16, no. 3, pp. 389–393, Jul. 2001.

[13] D. Kinh, S. Pham, R. Thomas, and E. Stinger Walt, "Analysis of stray current, track-to-earth potentials and substation negative grounding in DC traction electrification system," in *Proc. IEEE/ASME Joint Railroad Conf.*, Toronto, 2001, pp. 141–160.

[14] C. Charalambous, I. Cotton, and P. Aylott, "A simulation tool to predict the impact of soil topologies on coupling between a light rail system and buried third-party infrastructure," *IEEE Trans. Veh. Technol.*, vol. 57, no. 3, pp. 1404–1416, May 2008.

[15] T. J. Barlo and A. D. Zdunek, "Stray current corrosion in electrified rail systems—Final report," Infrastructure Technol. Inst., May 1995.

[16] P. Aylott, I. Cotton, and C. A. Charalambous, "Impact and management of stray current on DC rail systems," in *Proc. 4th IET Prof. Develop. Course Railway Electr. Infrastruct. Syst. Conf.*, May 2009, vol. 57, pp. 238–245.

Amr Ibrahem received the B.Sc. degree in electrical and electronic engineering from the University of Khartoum, Khartoum, Sudan, in 2012. He is currently working toward the M.Sc. degree in electrical engineering at the University of Akron, Akron, OH, USA.

His research interests include power electronics design for electric railway and renewable energy systems.

Ali Elrayyah received the B.Sc. degree in electrical and electronics engineering from the University of Khartoum, Khartoum, Sudan, in 2003, the M.Sc. degree in systems engineering from King Fahd University of Petroleum and Minerals, Dhahran, Saudi Arabia, in 2009, and the Ph.D. degree from the University of Akron, Akron, OH, USA, in 2013.

He is currently a Research Engineer with Qatar Research Foundation, Doha, Qatar. His research interests include alternative energy systems, and control of standalone and utility interactive energy systems.

Yilmaz Sozer (M'05–SM'14) received the B.S. degree in electrical engineering from Middle East Technical University Ankara, Ankara, Turkey, in 1993, and the M.S. and Ph.D. degrees in electric power engineering from Rensselaer Polytechnic Institute, Troy, NY, USA, in 1995 and 2000, respectively.

His masters and doctoral work focused on power electronics and the development of control algorithms for electric machines. He is currently an Associate Professor in the Electrical and Computer Engineering Department, University of Akron, Akron, OH, USA, involved in teaching and research. Before joining the University of Akron, he was with the Advanced Energy Conversion, Schenectady, NY. His research interests include control and modeling of electrical drives, alternative energy systems, design of electric machines, high-power isolated dc/dc converter systems, static power conversion systems that interface energy storage, and distributed generation sources with the electric utility.

Dr. Sozer has been involved in IEEE activities which support power electronics, electric machines, and alternative energy systems. He is serving as an Associate Editor for the IEEE TRANSACTIONS ON INDUSTRY APPLICATIONS and the IEEE TRANSACTIONS ON POWER ELECTRONICS. He is a Vice-Chair for the IEEE IAS Renewable and Sustainable Energy Conversion Systems Committee.

J. Alexis De Abreu-Garcia (M'86) received the B.S. and Ph.D. degrees in electrical engineering from Queen's University, Kingston, ON, Canada, in 1982 and 1986, respectively.

From 1985 to 1986, he was a Visiting Scientist with the Imperial College of Science and Technology, London, England, U.K. He joined the University of Akron, Akron, OH, USA, in 1987, where he is currently an ECE Professor. He chaired the ECE Department from 2000 to 2014, he was a Control Specialist in the Computer, Control and Electronic Technology Department, The Goodyear Tire and Rubber Company, from 1995 to 1996, and served as an Associate and Track Editor of the IEEE TRANSACTIONS ON INDUSTRIAL ELECTRONICS for more than 14 years. His research interests include control system analysis, design, and algorithms; order reduction of multidimensional large-scale linear, nonlinear, descriptor, and distributed parameter systems; classical and modern robust control techniques; system simulation; fuzzy/neurofuzzy logic control system design, modeling, and control of heart pumps, and smart materials. For the past several years, he has been working in sensors, especially in the power electronics and systems areas.